# Very Fast Transient Overvoltages in GIS with Compressed $SF_6$-$N_2$ Gas Mixtures

S. Singha and M. Joy Thomas

Department of High Voltage Engineering
Indian Institute of Science
Bangalore, India

## ABSTRACT

**This paper discusses the characteristics of very fast transient overvoltages (VFTO) in $SF_6$-$N_2$ gas mixtures at different percentages of $SF_6$. A comparison of the VFTO characteristics of pure $SF_6$ with those of pure $N_2$ is also presented. The investigations are performed using a laboratory model GIS bus duct having a test gap used for simulating a switching event leading to the generation of VFTO. A capacitive voltage sensor is used to measure the VFTO peak magnitude and temporal characteristics. Measurements were carried out at two different gap spacings (0.20 and 0.61 mm) over a pressure range of 100 to 500 kPa. VFTO characteristics for $N_2$, $SF_6$ and $SF_6$-$N_2$ mixtures obtained from the experiments show similar trends. The level of surge peak magnitude is <2.0 pu for all cases when the gap was 0.20 mm, but it reaches a maximum of 2.41 pu at 0.61 mm gap. At 0.20 mm gap, in $SF_6$-$N_2$ mixtures, the difference in peak magnitudes is not significant for 10% and 20% $SF_6$ mixtures (between 200 and 400 kPa) and also for pure $SF_6$ and 40% $SF_6$ (between 200 and 300 kPa). The occurrence of corona stabilization during breakdown of the gap may be the cause for such a behavior. Unlike the above observations at 0.20 mm gap, at 0.61 mm gap, the peak magnitudes strictly increase with pressure for the pure gases and gas mixtures. At 0.20 mm gap, the time to breakdown of the gap is found to be almost constant in all cases. But at 0.61 mm gap, the time to breakdown is seen to be dependent on the mixture, pressure, and breakdown voltage, and this observation is in accordance with Toepler's spark law.**

## 1 INTRODUCTION

$SF_6$ is the main insulating medium in almost all gas insulated HV equipment. However, in recent years, the future use of $SF_6$ is being debated throughout the world in spite of it having all the desirable properties of a good insulating and arc-quenching medium. When $SF_6$ is subjected to an electrical discharge, highly toxic and corrosive compounds are formed in small concentration [1]. It is also an efficient infrared (IR) absorber and hence a potent greenhouse gas [1]. The United Nations Convention on Climate Change has decided to reduce the emission quantity of greenhouse gases in 2010 to values lower than in 1990 [2]. Under this protocol, $SF_6$ gas also has to be reduced and therefore appropriate action is needed worldwide to replace $SF_6$ gas by environmentally friendly gases or gas mixtures. Due to the above reasons, investigations are in progress to develop alternative methods to minimize the release of $SF_6$ into the environment. Possible solutions are to use other gases or gas mixtures containing a lower content of $SF_6$. In this regard, $SF_6$-$N_2$ gas mixtures, containing different percentages of $SF_6$, have been found to be a good dielectric medium and is widely accepted as the best possible replacement for $SF_6$ [1]. The basic properties, behavior and performance of $SF_6$-$N_2$ mixtures as an insulating medium have been investigated thoroughly for several years in the past. Based on the research conducted worldwide, the optimum composition of $SF_6$-$N_2$ mixture (which can be used instead of $SF_6$ without requiring much change in hardware, operations or ratings of the existing GIS equipment) for practical applications is considered to be 40% to 60% $N_2$ mixture [1, 2]. Studies carried out in recent years also suggest that $SF_6$-$N_2$ mixture with $SF_6$ concentration as low as 20% can be used with an advantage. Even with low $SF_6$ content, this mixture has been found to exhibit many of the desirable properties of pure $SF_6$ [2].

Steep fronted transients, generally named very fast transient overvoltages (VFTO), are generated in GIS during operation of disconnector switches and circuit breakers or during a ground fault [3, 4]. At each irregularity of the characteristic impedance inside the GIS and its interfaces with other equipment, these transients are reflected and superimposed on the steady state voltage. Although these transients have a frequency band in a real GIS, a single frequency voltage shape has been used to evaluate the influence of VFTO on the dielectric behavior of the components in the GIS. With the advances in GIS technology, increasing emphasis is being given to the reliability of the disconnec-

1070–9878/1/ $3.00 © 2001 IEEE

tor switches and GIS components under the condition of fast transients. Earlier studies [3] have described the physical phenomena, which occur during disconnector switch arcing and the magnitude of the transients that occur. Also, the general requirements for disconnect and ground switches were discussed by Itoh *et al.* [5]. For the purpose of calculating transient magnitude, these authors and others have assumed a trapped charge of 1 pu prior to closing of the disconnect switch. The electromagnetic transients program (EMTP) has been used to calculate the transient magnitudes at various points within the GIS by modeling the different parameters on known lumped or distributed elements. The results thus obtained have shown that the transient magnitude can be as high as 2.5 pu.

The transient phenomena with respect to the overvoltage level (in pu) when pure $SF_6$ is used as the insulating medium in GIS has been extensively studied by analytical methods; experimental studies being rare. Experimental measurements of VFTO in a GIS with $SF_6$ insulation have been reported, but are mainly confined to the on-site testing of GIS [4, 6]. These experimental measurements were carried out using spherical electric field sensors that are capable of making non-contact measurements of the steep fronted voltage transients [4, 7, 8]. A majority of these measurements were made to confirm the adequacy of capacitive sensors in measuring VFTO in GIS systems and these reports contain more information on sensor performance and very less data pertaining to VFTO characteristics. It has been reported that the peak magnitude of the measured VFTO seldom exceeded 2.0 pu, but VFTO magnitudes >2.0 pu also have been reported [4, 8] in some other cases. The VFTO peak magnitude depends entirely on the GIS system layout in which experiments are conducted and thus the peak VFTO level will vary from system to system.

Also, under certain circumstances such as the presence of a trapped charge of 1 pu on the load side before disconnector operation and during occurrence of a ground fault, the VFTO level may reach 2.5 to 3.0 pu depending on the GIS system layout. In addition, experimental investigations have been undertaken to study the breakdown phenomena of a gap in a GIS with pure $SF_6$ and $SF_6$-$N_2$ gas mixtures under the application of very transient voltages [9, 10]. In most of these cases, fast transient voltages (mainly oscillating) were generated using a resonating test circuit and this was applied to the gap in a model GIS bus duct and the breakdown voltages were measured.

The time to breakdown of the gap in a GIS is reported to be normally between 4 to 20 ns depending on the field inhomogeneity and the peak of the transients has been reported to occur $\sim$ 200 ns after the gap has broken down [1]. The time for the occurrence of the maximum peak of the VFTO also depends mainly on the GIS system configuration.

Although some basic information is available on the characteristics of VFTO generated in a GIS using pure $SF_6$, detailed studies of the VFTO peak magnitudes and temporal characteristics by systematic variation of the gap distance, gas pressure and gas mixture over the practical pressure range in an actual GIS with $SF_6$-$N_2$ gas mixture as the insulating medium have not been reported yet.

Therefore, in the present study, experimental measurement of VFTO magnitude and temporal characteristics have been carried out in $SF_6$-$N_2$ mixtures at different gap spacings and gas pressures for mixture compositions varying from 10% to 40% $SF_6$ in $N_2$.

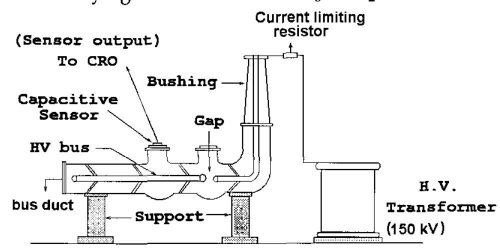


**Figure 1.** Experimental setup for measurement of VFTO characteristics.

## 2 EXPERIMENTAL TECHNIQUE

The experiments for the measurement of VFTO in $SF_6$-$N_2$ mixtures at different percentages of $SF_6$ in $N_2$ were carried out using a 145 kV GIS bus duct supplied by Siemens, Germany. The VFTO magnitudes were measured using a capacitive probe.

### 2.1 TEST GAP AND PROCEDURE

The experimental setup used in the present study is shown in Figure 1. Disconnector operation for the generation of VFTO was simulated by the breakdown of a 5 cm diameter hemispherical electrode gap, which is built into the model bus duct. VFTO characteristics at two different gaps of 0.20 and 0.61 mm were studied. For accurate measurement, and also to confirm the alignment of the electrode surfaces, the gap spacings were measured using a filler gauge to an accuracy better than $\pm$ 0.5%. Once the gap was adjusted, experiments for all mixture ratios and pressures were conducted without disturbing the gap. The GIS model bus duct is a single floating bus of length 2.45 m from the gap axis. Using the bus duct, experiments were carried out at each of the above mentioned gaps over a pressure range of 100 to 500 kPa. Pressure in the chamber was measured with the help of a pre-calibrated pressure gauge, which is inherent to the model bus duct and the pressures measured using this gauge are accurate to $\pm$ 2%. The HV bus was excited with a sinusoidal voltage of 50 Hz from a 150 kV HV test transformer. Over the range of voltages in the present study, the transformer is assumed to be discharge free. The model bus duct initially was evacuated to very low pressures of $\sim 10^{-3}$ kPa to remove air, moisture and other contaminants present. The duct was then filled with the appropriate gas in which experiments were performed. In case of pure $SF_6$ and pure $N_2$, cylinder grade gas (99.5% purity) was filled directly and left for $\sim$ 1 h before starting the experiments. For preparing $SF_6$-$N_2$ mixtures, the duct was filled according to the partial pressure of the gases. In this method, the gas having the lesser percentage content in the mixture, *i.e.* $SF_6$ in the present case is let in first followed by the gas with higher content in the mixture, *i.e.* $N_2$. The mixture was then left for a minimum of 5 h to allow proper mixing of the gases prior to start of the experiments. Between successive breakdowns, a time delay of $\sim$ 10 min was provided. The handling of $SF_6$ gas, *i.e.* evacuation, pressurizing and recycling *etc.* was done with the help of a gas recycling and pressurizing plant from DILO, Germany.

### 2.2 MEASURING SYSTEM

The VFTO were measured using a capacitive voltage sensor having a fast response time, which was developed in-house specifically for this purpose [11]. The voltage rise time of the sensor (the time to rise from 10% to 90% of the full amplitude) is sufficiently steep for measuring the voltage rise of a disconnector induced fast transient. The fast transients generated due to the breakdown of the gap are recorded on an oscilloscope (200 MHz Tektronix digital storage oscilloscope having a sampling rate of 1 Gsample/s), which was connected from the output of the sensor using a 0.6 m long coaxial cable (RG58/CU). It was found through simulation that the connecting cable would not induce any effect on the VFTO characteristics. Also, since the objective of the measurement was on the pu value of the VFTO peak (*i.e.* the ratio of the peak voltage to the actual 50 Hz ac peak voltage) rather than the actual voltage levels, the possible error in measurement of the pu peak of the VFTO using the oscilloscope can be neglected. The VFTO waveforms were recorded at an appropriate time sweep taking into consideration the accuracy with which the parameters of the plot can be measured on the CRO screen. A schematic of the sensor used for measurement is shown in Figure 2.

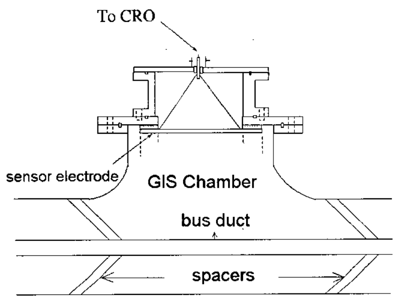


**Figure 2.** Capacitive sensor used for measurements.

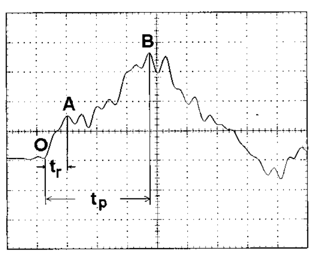


**Figure 3.** A typical VFTO waveform. Time Scale: 2.5 ns/div. $t_r$ = Breakdown time. $t_p$ = time to maximum peak. O: is at 10% of the peak value (B) obtained with zero (0 V) as the base. A: is the first peak from O on the rising portion of the VFTO waveform. B: maximum peak of the VFTO

Using the experimental technique described above, it was possible to measure the VFTO characteristics in the GIS model bus duct with $SF_6$-$N_2$ gas mixture insulation up to an accuracy of ± 2%. A typical VFTO waveform recorded using the experimental setup is shown in Figure 3 where the different parameters of interest are shown. The results and discussions are presented in the following Sections.

## 3 RESULTS

Typical VFTO characteristics recorded at a pressure of 500 kPa using the experimental setup described above for pure $N_2$, pure $SF_6$ and mixtures of $SF_6$ in $N_2$ with concentrations of 10%, 20% and 40% are shown in Figures 4, 5 and 6. Only characteristics at a pressure of 500 kPa are shown because it lies in the practical pressure range of a GIS filled with pure $SF_6$. The characteristics at other gas pressures are similar to the ones shown. Figures 4 and 5 show the characteristics obtained at gaps of 0.20 mm and 0.61 mm respectively, while characteristics in Figure 6 correspond to those recorded at 0.61 mm gap, but at shorter time scales. In addition, the results of the VFTO rise times and the overvoltage factor (in pu) for the pure gases as well as the gas mixtures at all pressures are given in Table 1 for both 0.20 and 0.61 mm gaps. These data are shown in Figure 7 as variations of the overvoltage factor with gas/mixture pressure, while the same data are shown in Figure 8 as a function of $SF_6$ concentration in $N_2$.

It can be seen from Figure 7 that the overvoltage factor increases with the gas/mixture pressure for the two gaps studied. It is evident from Figure 8 that the overvoltage factor is lowest in $N_2$ and increases with increase in $SF_6$ concentration. The characteristics clearly exhibit a nonlinear trend, which is more pronounced at higher gas pressures (400 and 500 kPa). Between 300 and 500 kPa, there is a rapid increase in the overvoltage factor to $\lesssim$40% $SF_6$ content in $N_2$ (at 0.61 mm gap) but only to 10% $SF_6$ (at 0.20 mm gap). Between pressures of 200 and 300 kPa at 0.20 mm gap, there is no significant difference in the overvoltage factors for pure $SF_6$ and 40% $SF_6$ in $N_2$ mixture. A similar observation is seen for the mixtures having 20% and 10% $SF_6$ in $N_2$, but now between 200 and 400 kPa. On the other hand, at 0.61 mm gap, such observations could not be made.

As can be seen from Figures 4, 5 and 6 and also from Table 1, at 0.20 mm gap, the time to breakdown of the gap is almost constant at 5.5 ns for pure $SF_6$ and its mixtures at all pressures, while it is 6.0 ns for $N_2$ to 400 kPa pressure. On the contrary, with 0.61 mm gap, the breakdown time of the gap is seen to decrease with increasing pressure as well as breakdown voltage. The lowest sparking time observed was 3.4 ns for $SF_6$ at 500 kPa as can be seen clearly from Figure 6. Most of these data are obtained for the first time, and wherever possible comparisons have been made with published data.

## 4 DISCUSSION

For the sake of clarity, the results obtained at the two gap spacings at gas/gas mixture pressures ranging from 100 to 500 kPa and for different gas mixture ratios are analyzed and discussed under appropriate Sections.

### 4.1 WAVEFORMS

From the typical VFTO waveforms shown in Figures 4, 5 and 6, it can be seen that the VFTO waveforms are similar to those obtained earlier during studies on GIS systems using fast response capacitive sensors [4]. It has a steep initial rise (3 to 6 ns), a peak that does not occur in the steepest portion of the wave, and a gradually decaying oscillating component. It can be observed further that the waveforms are all similar

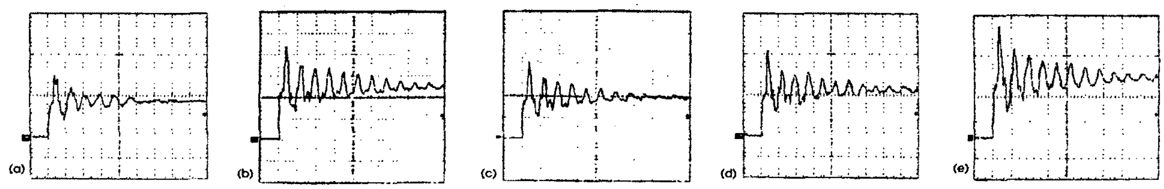


**Figure 4.** VFTO Characteristics at 500 kPa for 0.20 mm gap. Divider ratio = 456± 2 [9]. (a) Pure $N_2$ [Scale: 7 V/div, 50 ns/div], (b) 10% $SF_6$–90% $N_2$ [Scale: 8 V/div, 50 ns/div], (c) 20% $SF_6$–80% $N_2$ [Scale: 10 V/div, 50 ns/div], (d) 40% $SF_6$–60% $N_2$ [Scale: 10 V/div, 50 ns/div], (e) Pure $SF_6$ [Scale: 10 V/div, 50 ns/div].

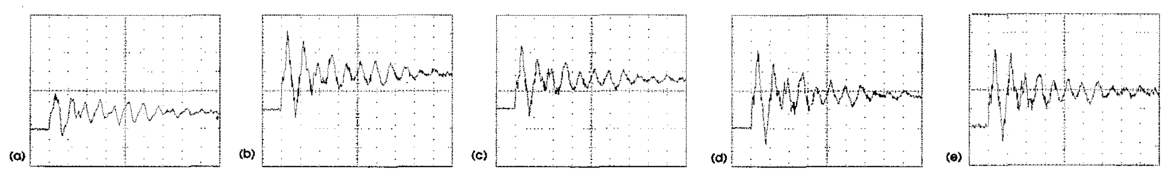


**Figure 5.** VFTO Characteristics at 500 kPa for 0.61 mm gap. Divider ratio = 456± 2 [9]. (a) Pure $N_2$ [Scale: 5 V/div, 50 ns/div], (b) 10% $SF_6$–90% $N_2$ [Scale: 5 V/div, 50 ns/div], (c) 20% $SF_6$–80% $N_2$ [Scale: 7 V/div, 50 ns/div], (d) 40% $SF_6$–60% $N_2$ [Scale: 5 V/div, 50 ns/div], (e) Pure $SF_6$ [Scale: 5 V/div, 50 ns/div].

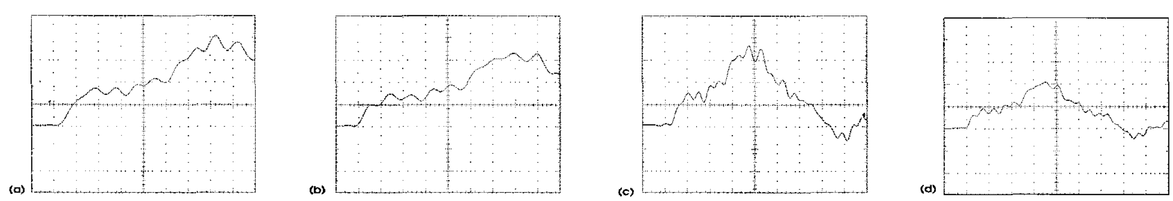


**Figure 6.** VFTO Characteristics at shorter time scales at 500 kPa for 0.61 mm gap. Divider ratio = 456± 2 [9]. (a) 10% $SF_6$–90% $N_2$ [Scale: 5 V/div, 2.5 ns/div], (b) 20% $SF_6$–80% $N_2$ [Scale: 7 V/div, 2.5 ns/div], (c) 40% $SF_6$–60% $N_2$ [Scale: 5 V/div, 5 ns/div], (d) Pure SF6 [Scale: 10 V/div, 5 ns/div].

irrespective of any variations in the gap spacings, mixture concentrations and gas pressures. This observation is due to the fact that the nature of the VFTO waveform depends on the GIS configuration and in the present study, VFTO measurements were carried out using the same GIS bus duct configuration for all the cases.

## 4.2 VFTO CHARACTERISTICS - OVERVOLTAGE FACTOR

It can be seen from Figures 7 and 8 that the VFTO magnitudes increase with increasing gas/gas mixture pressure and with increasing concentration of $SF_6$ in $N_2$. The maximum magnitude recorded was 2.41 pu in 0.61 mm gap at 500 kPa. At 0.20 mm gap, the increase in the overvoltage factors is almost linear over the complete pressure range studied while for 0.61 mm gap, linearity is observed to $\leqslant$300 kPa only (Figure 7). For a given system configuration, the VFTO magnitudes depend on the breakdown voltage of the gap. Since the breakdown voltage of the gap increases with increasing gas pressure and concentration of $SF_6$ in the gas mixture, the VFTO magnitude also increases accordingly. The VFTO peak magnitudes in $N_2$ are lower compared to those in pure $SF_6$ and $SF_6$-$N_2$ gas mixtures at all gas pressures and at both gaps studied, which is due to the correspondingly lower values of the breakdown voltages for $N_2$ compared to those of pure $SF_6$ and $SF_6$-$N_2$ mixtures.

The VFTO magnitude was observed to increase rapidly on increasing the percentage of $SF_6$ from 0 to 10% in the mixture at all pressures (Figure 8). However, with the further addition of $SF_6$ in $N_2$, the rate of rise in the VFTO magnitude reduces at all pressures. The trends in the variations of overvoltage factors with mixture compositions are distinctly different at the two gaps studied. At 0.20 mm gap, the rapid increase in VFTO magnitude to $\leqslant$10% $SF_6$ concentration occurs at all pressures, but it is pronounced at higher pressures. Further increase in $SF_6$ concentration appears to have no significant effect on the overvoltage factors especially at lower pressures. On the other hand, at the gap distance of 0.61 mm, the overvoltage factor increases linearly with the $SF_6$ concentration to $\leqslant$20% (100 and 200 kPa) and increases more rapidly with increasing $SF_6$ concentration in the mixture (especially at 200 kPa). At pressures >300 kPa, the increase in overvoltage factor is rapid when the $SF_6$ concentration was increased from 0% to 40% and it is less steep at $SF_6$ concentrations >40%. The variations of the VFTO magnitudes at both gap spacings are also similar to the variations obtained in the attachment coefficient $(\eta/p)$ *vs.* % $SF_6$ in $N_2$ characteristics [12]. The difference between the VFTO magnitudes obtained in various mixtures is lower at lower pressures and higher at 400 and 500 kPa. Table 1 shows the differences in the VFTO magnitudes for different gas mixtures. In both gaps, the breakdown process mostly controls the variations in the overvoltage factor.

**Table 1.** Time to breakdown and VFTO magnitudes at different pressures and gap spacings. $t_r$ is the breakdown time.

| Pressure | pure $SF_6$ | | $40\%SF_6$-$60\%N_2$ | | $20\%SF_6$-$80\%N_2$ | | $10\%SF_6$-$90\%N_2$ | | Pure $N_2$ | |
|---|---|---|---|---|---|---|---|---|---|---|
| | $t_r$ | VFTO | $t_r$ | VFTO | $t_r$ | VFTO | $t_r$ | VFTO | $t_r$ | VFTO |
| kPa | ns | pu | ns | pu | ns | pu | ns | pu | ns | pu |
| Gap spacing 0.61 mm | | | | | | | | | | |
| 100 | 4.20 | 1.91 | 4.30 | 1.89 | 4.35 | 1.80 | 4.50 | 1.77 | 5.50 | 1.74 |
| 200 | 4.10 | 2.19 | 4.15 | 1.95 | 4.25 | 1.82 | 4.28 | 1.80 | 5.40 | 1.77 |
| 300 | 3.95 | 2.33 | 3.98 | 2.19 | 4.05 | 2.02 | 4.08 | 1.95 | 5.32 | 1.88 |
| 400 | 3.80 | 2.37 | 3.85 | 2.30 | 3.93 | 2.18 | 4.02 | 2.06 | 5.25 | 1.92 |
| 500 | 3.40 | 2.41 | 3.60 | 2.34 | 3.70 | 2.23 | 3.95 | 2.15 | 5.20 | 2.04 |
| Gap spacing 0.2 mm | | | | | | | | | | |
| 100 | 5.5 | 1.66 | 5.5 | 1.65 | 5.5 | 1.62 | 5.5 | 1.59 | 6.0 | 1.58 |
| 200 | 5.0 | 1.71 | 5.5 | 1.70 | 5.5 | 1.68 | 5.5 | 1.67 | 6.0 | 1.64 |
| 300 | 5.0 | 1.75 | 5.5 | 1.74 | 5.5 | 1.72 | 5.5 | 1.71 | 6.0 | 1.65 |
| 400 | 5.0 | 1.83 | 5.0 | 1.75 | 5.0 | 1.73 | 5.5 | 1.72 | 6.0 | 1.66 |
| 500 | 5.0 | 1.88 | 5.0 | 1.82 | 5.0 | 1.78 | 5.5 | 1.77 | 5.5 | 1.67 |

At 0.20 mm gap (see Figure 7), the variation in VFTO magnitude in pure $SF_6$ and in all the gas mixtures studied is similar (but ill defined) to the non-uniform field breakdown due to corona stabilization observed earlier [13]. The VFTO magnitude increases very rapidly when the $SF_6$ concentration in $N_2$ increases from 0% to 10% (Figure 8). But it is interesting to note that there is negligible difference in the VFTO magnitudes between mixtures containing 10% and 20% $SF_6$ (200 to 400 kPa) and also between 40% and 100% $SF_6$ (200 to 300 kPa) (Figure 7). A possible reason for such an observation may be due to the occurrence of corona stabilization in the gap (at 0.20 mm). In the present investigations, hemispherical electrodes were used and experiments were carried out at small gap distances. But some roughness on the electrode surfaces have been observed due to surface erosion over a small area near the tip of the electrodes. These small surface irregularities become more prominent when very small gaps are used for experiments (since the discharge area is reduced) and thus the occurrence of corona stabilized breakdown of the gap cannot be ruled out. Since the gap distance at 0.20 mm gap is very small, it is felt that the corona stabilization effect could be the reason behind such an observation. It may be emphasized here that a similar observation is not seen in the case of pure $N_2$ (0.20 mm gap in Figure 7). Moreover, this effect is not seen with the 0.61 mm gap (Figure 8), and the VFTO magnitudes are distinct at different gas pressures. This may be due to the reason that because of the slightly larger gap at 0.61 mm (compared to 0.20 mm), the discharge area has increased and the surface non-uniformity does not contribute to the breakdown process (*i.e.* corona stabilization does not take place).

## 4.3 TIME TO GAP BREAKDOWN

With respect to the time to breakdown of the gaps, two different observations have been made for the two gap distances investigated. It can be observed from Table 1 that the time to breakdown at 0.20 mm gap remains practically constant in the range of 5 to 6 ns irrespective of changes in the gas pressures at different gas mixture ratios. The time to breakdown has been observed to be constant at 5.0 ns (in pure $SF_6$) and 5.5 ns (10% $SF_6$ in $N_2$), while in gas mixtures containing 20%, it remains constant at 5.5 ns until 300 kPa and reduces to 5.0 ns at 400 and 500 kPa. Only in the case of $N_2$, the breakdown time is slightly higher at 100 kPa compared to its value at 500 kPa. These observations are in close agreement with the results of Pfeiffer [14], which shows that for approximately uniform fields and small gap separations, the difference

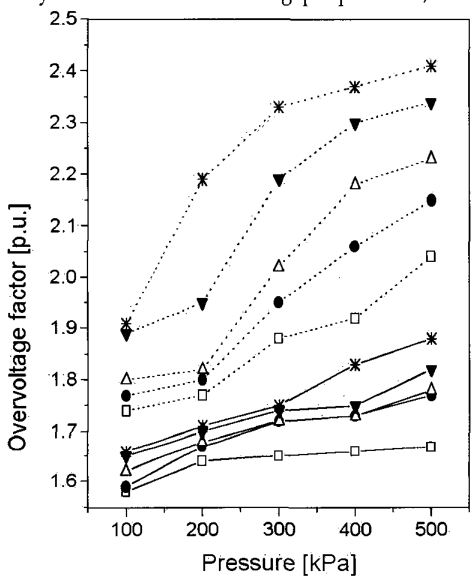


**Figure 7.** Pressure *vs.* overvoltage factor characteristics for both the gaps. □: pure $N_2$, ●: 10% $SF_6$–90% $N_2$, △: 20% $SF_6$–80% $N_2$, ▼: 40% $SF_6$–60% $N_2$, ★: pure $SF_6$. Dotted lines in the graph pertain to data at a gap of 0.61 mm. Solid lines are for a gap of 0.20 mm.

in the time lags (formative time) between $N_2$ and $SF_6$ does not seem to be very important. This is true for the case of $SF_6$-$N_2$ mixtures as observed in the present investigations. At this small gap (0.20 mm), the formative time lags to breakdown will be very small irrespective of the gaseous medium and therefore the contribution of the formative time lags to the total breakdown time of the gap is negligible.

Contrary to the above observation, the breakdown time in the case of 0.61 mm gap has been found to be varying with respect to the gas pressure and $SF_6$ concentration in $N_2$ (Table 1). The breakdown time decreases with increasing gas pressure and $SF_6$ concentration in $N_2$ and the shortest breakdown time (3.4 ns) has been observed at 500 kPa for pure $SF_6$. Therefore, the time to breakdown is a function of the gas pressure and the $SF_6$ concentration in $N_2$ in the 0.61 mm gap. This observation has been found to agree with Toepler's spark law (commonly

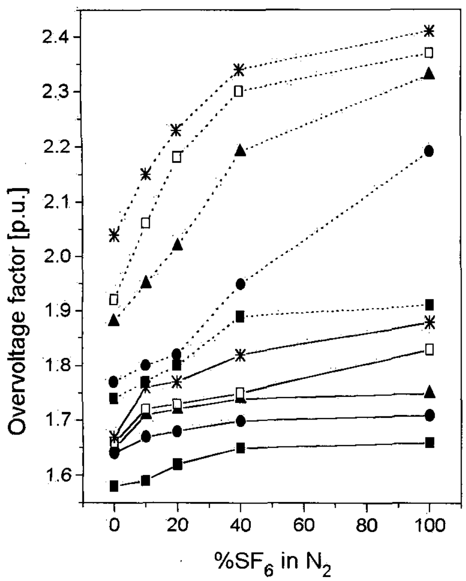


**Figure 8.** % $SF_6$ in $N_2$ *vs.* overvoltage factor characteristics for both the gaps. ■: 100 kPa, ●: 200 kPa, ▲: 300 kPa, □: 400 kPa, ★: 500 kPa. Dotted lines in the graph pertain to data at a gap of 0.61 mm. Solid lines are for a gap of 0.20 mm.

used to explain VFTO phenomena in GIS [3]). According to Toepler's empirical relation [3, 15], the time to breakdown of the gap (or the rise time of the VFTO) is inversely proportional to the breakdown voltage of the gap. Since the breakdown voltage of the gap increases with increasing gas pressure and $SF_6$ concentration in $N_2$, the time to breakdown of the gap correspondingly decreases. Although Toepler's law explains the change in rise time with the breakdown voltage, only varying Toepler's constant with respect to the gas/gas mixture pressure and concentration can account for the changes in the breakdown time at 0.61 mm gap in the present study (Table 1).

### 4.4 TIME TO PEAK OF THE VFTO

It can be observed from Figures 4, 5 and 6 that the maximum peak of the VFTO in pure $SF_6$, pure $N_2$ and mixtures of $SF_6$ and $N_2$ at different gas mixture pressures and mixture concentrations occur after a certain time, which is $\sim$ 17 to 18 ns. The same observations were made at 0.20 mm gap. The occurrence of the maximum peak is related to the reflections of the voltage wave from impedance mismatches and other terminations in the GIS bus duct. The GIS bus duct used in the current experiments is a single floating bus of length 2.45 m from the test gap and it remains unaltered for all experimental sets. Since the length of the bus is constant and there are no impedance mismatches, except for the presence of spacers (Figure 1), the peak of the voltage wave occurs at the first reflection from the end of the bus. The travel time for the first reflection of the voltage wave generated in the test gap from the end of the floating bus will be

$$t = \frac{2l}{v} \qquad (1)$$

where $l$ is the length of the bus, and $v$ the velocity of propagation of the voltage wave.

Assuming a velocity of propagation 0.95× the speed of light (due to the presence of spacers, *etc.*), the travel time of the voltage wave generated after breakdown of the gap in the GIS to get reflected is $\approx$ 17.2 ns, which is comparable to the time obtained from the experiments.

## 5 CONCLUSIONS

In the present study, VFTO characteristics in a GIS with $SF_6$-$N_2$ gas mixture (at different percentages of $SF_6$) as the insulating medium were recorded and the overvoltage factors were measured. A 50 Hz ac voltage source was used for triggering the gas gap within the GIS bus duct. Results have shown that the VFTO magnitude in $N_2$, $SF_6$ and its mixture increase with increasing concentration of $SF_6$ in $N_2$. At 0.20 mm gap, the overvoltage factors were found to increase rapidly on addition of 10% $SF_6$ in $N_2$ but at higher pressures. On the other hand, at 0.61 mm gap, the overvoltage factor increases rapidly to $\leqslant$40% $SF_6$ concentration especially at higher mixture pressures. At 0.20 mm gap, between 200 and 400 kPa, there is an indication of the occurrence of corona stabilization in the breakdown process for different mixture ratios. But this effect is not seen at 0.61 mm gap and the overvoltage factors strictly increase with pressure. Thus, it appears that variations in the overvoltage factor for the pure gases and gas mixtures at both the gaps are directly related to the breakdown process. No significant change in the rise time of the VFTO could be observed for pure $N_2$, pure $SF_6$ and its mixtures at 0.20 mm gap. This is because of the fact that the formative time lags in all cases under the experimental conditions of the present study do not play any important role in the discharge growth. But, at 0.61 mm gap, similar observation could not be made, and the formative time and hence the Toepler's constant is a function of the gas/mixture pressure, breakdown voltage and mixture concentration.

From Table 1, considering the overvoltage factors at 400 and 500 kPa (working pressure range in a GIS) for both gap spacings, it can be noted that the percentage decrease in the VFTO magnitudes for 10% and 20% $SF_6$ in $N_2$ mixture at 500 kPa is quite significant compared to pure $SF_6$. Thus, bearing the overvoltage factor in mind, it appears that 10% to 20% $SF_6$ mixture concentration is better suited for application in gas insulated systems. But, from the point of view of the dielectric strength, a compromise has to be made with the operational pressure and the dimensions of the GIS apparatus and in this respect such a mixture ratio may prove insufficient. The use of lower $SF_6$ concentration mixtures in GIS will no doubt reduce the use of $SF_6$ gas, which is costly and also harmful for the environment, but problems will still exist with respect to the maintenance of a uniform gas mixture ratio and the removal and recycling of the gas mixture.

## REFERENCES


[1] L. G. Christophorou, J. K. Olthoff and D. S. Green, "Gases for Electrical Insulation and Arc Interruption: Possible, Present and Future Alternatives to pure $SF_6$", NIST Technical Note 1425, November 1997.

[2] L. G. Christophorou and R. J. Van Brunt, "$SF_6$-$N_2$ Mixtures: Basic and HV Insulation Properties", IEEE Transactions on Dielectrics and Electrical Insulation, Vol. 2, No. 5, pp. 952–1003, October 1995.

[3] S. A. Boggs, F. Y. Chu, N. Fujimoto, A. Krenicky, A. Plessl and D. Schlicht, "Disconnect Switch Induced Transients and Trapped Charge in a GIS", IEEE Trans. on Power Apparatus and Systems, Vol. 101, No. 10, pp. 3593–3602, October 1982.

[4] J. Meppelink, K. Diederich, K. Feser and W. Pfaff, "Very Fast Transients in GIS", IEEE Transactions on Power Delivery, Vol. 4, No. 1, pp. 223–233, January 1989.

[5] N. Itoh, Y. Marayama, S. Ohyama and S. Takeshita, "Switching Requirements for Disconnecting Switch and grounding Switch of GIS", *Surges in HV Networks*, K. Ragaller (ed.), Plenum Publishers, 1980.

[6] J. Lewis, B. M. Pryor, C. J. Jones and T. Irwin, "Disconnector operations in Gas Insulated Substations, overvoltage studies and tests associated with a 420 kV installation", CIGRE, Vol. II, paper 33. 09, pp. 1–8, 1988.

[7] S. A. Boggs and N. Fujimoto, "Techniques and Instrumentation for Measurement of Transients in Gas Insulated Switchgear", IEEE Transactions on Electrical Insulation, Vol. 19, No. 2, pp. 87–92, April 1984.

[8] H. Murase, I. Ohsima, H. Aoyagi and I. Miwa, "Measurement of Transient Voltages Induced by Disconnect Switch Operation", IEEE Trans. on Power Apparatus and Systems, Vol. 104, No. 1, pp. 157–165, January 1985.

[9] Hyeong-Ho Lee, Jin-Gi Kim, Ik-Soo Kim, Jong-Yeon Kim and Sang-Jin Jung, "Experimental Investigations of Very Fast Transient Overvoltages in GIS", Proceedings of 9th ISH, Graz, pp. 6783(1)–6783(4), Aug. 28–Sep. 1, 1995.

[10] William Pfeiffer, D. Schoen and C. Zender, "Corona Stabilization in $SF_6/N_2$ Mixtures under VFT stress", Proceedings of 11th ISH London, pp. 3.84. S18–3.87. S18, 23–27 Aug. 1999.

[11] V. Vinod Kumar and Joy Thomas M., "Capacitive sensor for the measurement of VFTO in GIS", Proc. of 11th ISH, London, pp. 1. 156. P4–1. 159. S6, 23–27 Aug. 1999.

[12] M. C. Siddagangappa, C. S. Lakshminarasimha and M. S. Naidu, "Ionization and attachment in binary mixtures of $N_2$-$SF_6$ and $N_2$-$CCl_2F_2$", J. Phys. D: Appl. Phys., Vol. 16, pp. 763–772, 1983.

[13] O. Farish, "Corona-controlled Breakdown in $SF_6$ and $SF_6$ Mixtures", Proc. of XVI International Conference On Phenomena in Ionized Gases, Dusseldorf, West Germany, pp. 187–195, 1983.

[14] W. Pfeiffer, "Time Characteristics and Breakdown Development for Steep-fronted Pulses", *Gaseous Dielectrics*, Volume IV, L. G. Christophorou (Ed.), pp. 323–334, 1984.

[15] W. Pfeiffer, "Spark Development in Compressed Gases (in German)", z. angew. Physik, Vol. 32, pp. 265–273, 1971.

*Manuscript was received on 25 March 2000, in revised form 23 February 2001.*